This is the post print version of the article, which has been published in Journal of trace elements in medicine and biology . 2018, 48, 149-156. http://dx.doi.org/ 10.1016/j.jtemb.2018.03.014 .

GENE EXPRESSION IN ADVERSE REACTION TO METAL DEBRIS AROUND METAL-ON-METAL ARTHROPLASTY: AN RNA-SEQ-BASED STUDY

Short title: Gene expression in adverse reaction to metal debris: an RNA-Seq study

Antti Pemmari[1], Tiina Leppänen[1], Erja-Leena Paukkeri[1], Antti Eskelinen[2], Teemu Moilanen[1,2] and Eeva Moilanen[1]*

[1]The Immunopharmacology Research Group, Faculty of Medicine and Life Sciences, University of Tampere and Tampere University Hospital, Tampere, Finland

[2]Coxa Hospital for Joint Replacement, Tampere, Finland

* Corresponding author

eeva.moilanen@staff.uta.fi (EM)

Mailing address:

University of Tampere

Faculty of Medicine and Life Sciences

Arvo-Building

Arvo Ylpön katu 34

33014 Tampere

Finland

Abstract

Joint replacement surgery is a standard treatment of advanced osteoarthritis (OA). Since 2000, cobalt-chromium (CoCr) metal-on-metal (MoM) implants were widely used in hip arthroplasties. Some patients developed “adverse reaction to metal debris” (ARMD) around the prosthesis resulting in a need for revision surgery. In the present study, we addressed the pathogenesis of ARMD by genome-wide expression analysis.

Pseudosynovial ARMD tissue was obtained from revision surgery of Articular Surface Replacement (ASR, DePuy, Warsaw, IN, USA) hip arthroplasties. Control tissue was 1) OA synovium from primary hip arthroplasties and 2) inflammatory pseudosynovial tissue from metal-on-plastic (MoP) implant revisions.

In ARMD tissue, the expression of 1446 genes was significantly increased and that of 1881 decreased as compared to OA synovium. Genes associated with immune response, tissue development and certain leukocyte signaling pathways were enriched in the differently (FC >2) expressed genes. The network analysis proposed PRKACB, CD2, CD52 and CD53 as the central regulators of the greatest (FC >10) differences.

When ARMD tissue was compared to MoP tissue, the expression of 16 genes was significantly higher and that of 21 lower. Many of these genes were associated with redox homeostasis, metal ion binding and transport, macrophage activation and apoptosis. Interestingly, genes central to myofibroblast (AEBP1 and DES) and osteoclast (CCL21, TREM2 and CKB) development were upregulated in the MoP tissue. In network analysis, IL8, NQO1, GSTT1 and HMOX1 were identified as potential central regulators of the changes.

In conclusion, excessive amounts of CoCr debris produced by MoM hip implants induces in a group of patients a unique adverse reaction characterized with enhanced expression of genes associated with inflammation, redox homeostasis, metal ion binding and transport, macrophage activation and apoptosis.

Keywords: joint replacement; adverse reaction to metal debris; metal-on-metal implant; metal-on-plastic implant; RNA-Seq

Introduction

Total hip joint replacement surgery is a standard treatment for advanced osteoarthritis (OA), rheumatoid arthritis (RA) and hip fracture [1–3]. During the first decade of the 21st century, metal-on-metal (MoM) implants were widely used in these operations, aiming at increased mechanical durability compared to the conventional metal-on-plastic (MoP) implants [4,5]. However, a part of the patients developed adverse inflammatory reactions around the implant, requiring revision surgery. Named "adverse reaction to metal debris" (ARMD), these reactions are characterized by marked inflammation and, in some cases, pseudotumor formation [6,7].

The ARMD reaction is thought to be caused by metal, especially cobalt, ions and nanoparticles abraded from the implant [8,9], but the detailed pathogenesis of the reaction remains unknown. However, it has been shown to include systemic dissemination of metal ions and nanoparticles, increased oxidative stress, inflammation, DNA damage and coagulative necrosis [10–12].

Lymphocytes and macrophages are predominant cell types in ARMD reaction [6,13]. Metal ions may act as haptens, activating T cells and eliciting a delayed hypersensitivity reaction (type IV immune response) [14]. Their direct cytotoxic effects can also cause tissue necrosis, which in turn may attract macrophages and lead to granulomatous responses [15] and osteolysis [16]. Cobalt may also stimulate macrophages through direct activation of Toll-like receptor 4 (TLR4) [17] and/or so-called danger signaling [18].

Reactions observed around a failed MoP implants share many features of the ARMD reaction. They are characterized by lymphocytic inflammation [19], macrophage activation, differentiation of mononuclear cells into osteoclasts and subsequent osteolysis [20]. These reactions are thought to be driven by implant-derived polyethylene particles [21], which can elicit inflammation and osteolysis in *in vitro models* [22].

In the present study, we approached the pathogenesis of the ARMD reaction by genome-wide expression analysis, with a special focus on differences between ARMD tissue and the inflammatory response around failed MoP joints.

Materials and methods

Patients

The study was approved by the Ethics Committee of Tampere University Hospital, Tampere, Finland, and complies with the declaration of Helsinki. All patients provided their written informed consent. Pseudotumor tissue from ten revision surgeries of Articular Surface Replacement (ASR) XL hip implants (DePuy, Warsaw, IN, USA) were collected and analyzed. Control samples of pseudosynovial tissue were collected from six revision operations of failed metal-on-plastic (MoP) joints and synovial samples from five OA patients in primary total hip arthroplasties. All operations were carried out at Coxa Hospital for Joint Replacement, Tampere, Finland, and all primary arthroplasties had been performed for the treatment of end-stage osteoarthritis.

Reasons for Revision Surgery

Revision surgeries of MoM hips were performed for one (or more) of the following indications: 1) a pseudotumour, either with a solid core or atypical contents, was seen in the vicinity of the implant, regardless of symptoms and whole blood metal ion levels; or 2) the patient had both elevated metal ion levels and hip symptoms despite a normal finding on cross-sectional imaging; or 3) the patient had an increasingly and significantly symptomatic hip regardless of imaging findings or metal ion levels. Symptoms included hip pain, discomfort, sense of instability, and/or impaired function of the hip as well as sounds from the hip. Infection was ruled out by at least five bacterial cultures obtained during revision surgery. The revision surgeries of MoP hips were performed for either aseptic loosening of the implants or for recurrent dislocation of the hip. The MoP implants included various brands and had been in-situ for a minimum of one year.

Tissue processing and RNA extraction

Peri-implant tissue was obtained directly from surgery. Necrotic mass (if present) was removed, and the tissue was cut into pieces weighing approximately 100 mg and the tissue samples were stored in 1000 µl of

RNA*later*™ solution (Thermo Fisher Scientific, Waltham, MA, USA). The samples were centrifuged, supernatant removed, and the samples were homogenized in QIAshredder™ columns (Qiagen). Total RNA was extracted using RNeasy Mini Spin columns (Qiagen) and treated with DNAse (Fermentas UAB, Vilnius, Lithuania).

Next-generation sequencing and data analysis

Sequencing of the RNA samples was performed in the Turku Centre of Biotechnology sequencing core, Turku, Finland, using the Illumina HiSeq 2500 sequencing platform. Sequencing depth was 20 million single-end reads with length of 50 base pairs (bp). The data was analyzed using the automated TRAPLINE RNA-Seq data analysis workflow [23] implemented on the Galaxy platform [24]. In brief, the reads were trimmed for quality, and read quality was assessed using FastQC [25]. The reads were aligned to a reference human genome using TopHat2 [26], and differential expression was assessed with Cufflinks [27]. For the purposes of further analysis, genes with an expression fold change (FC) > 2.0 in either direction and false discovery rate (FDR)-corrected p-value < 0.05 were deemed biologically and statistically significant. Functions of the genes were obtained from the NCBI Gene database, if not otherwise indicated. Mean gene expression levels are reported as reads per kilobase per million (RPKM) values. Functional analysis from the Gene Ontology (GO) database [28] was performed using the DAVID tool [29], and the resulting list was reduced using REVIGO [30]. Protein interactions were studied with STRING [31].

Results

When comparing ARMD tissue to OA tissue, the expression of 1446 genes was found to be significantly higher and that of 1881 genes significantly lower in the former. Of these, 622 genes had a positive expression fold change (FC) of more than 2.0, and 528 a negative one of similar magnitude. Tables 1 and 2 show 20 genes with the greatest FCs into both directions, along with their functions potentially relevant for the metal debris-induced reaction. These can be seen to encompass a wide variety of different actions, especially lymphocyte and macrophage-mediated inflammatory response, tissue development, redox homeostasis and cellular metabolism.

Table 1: 20 genes with the highest expression levels in ARMD compared to OA tissue. Gene expression levels in adverse reaction to metal debris (ARMD) and osteoarthritis (OA) samples are listed as reads per kilobase million (RPKM) values, and the differences as fold changes (FCs). *p*-values are adjusted by false discovery rate (FDR).

Gene	Name	Function	RPKM (ARMD)	RPKM (OA)	FC	adj. *p*
TNFRSF14	TNF receptor superfamily member 14	T-cell mediated immunity	61.09	0.20	**307.19**	0.0018
FAM213B	Family with sequence similarity 213 member B	Prostaglandin synthesis	271.81	1.14	**239.05**	0.00043
KCNAB2	Potassium voltage-gated channel subfamily A regulatory beta subunit 2	Potassium transport	18.57	0.10	**184.80**	0.042
PGD	Phosphogluconate dehydrogenase	Pentose phosphate shunt	33.22	0.22	**153.04**	0.014
PEX14	Peroxisomal biogenesis factor 14	Peroxisome production	3452.48	42.31	**81.59**	0.00043
AGTRAP	Angiotensin II receptor associated protein	Regulation of vascular tone	187.96	2.44	**77.09**	0.00043
MIIP	Migration and invasion inhibitory protein	Regulation of cell migration	16.12	0.24	**66.56**	0.00043
TMEM51	Transmembrane protein 51	Membrane component	54.35	0.96	**56.90**	0.00043
EFHD2	EF-hand domain family member D2	Regulation of cell migration	48.94	0.88	**55.36**	0.00043
PLEKHM2	Pleckstrin homology and RUN domain containing M2	Organelle localization	128.21	2.63	**48.69**	0.00043
NECAP2	NECAP endocytosis associated 2	Endocytosis	45.97	0.99	**46.31**	0.00043
ARHGEF10L	Rho guanine nucleotide exchange factor 10 like	Signal transduction	55.92	1.37	**40.81**	0.00043
C1QA	Complement C1q A chain	Innate immunity	16.80	0.43	**38.84**	0.00043
PITHD1	PITH domain containing 1	Regulation of gene expression	1916.92	54.85	**34.95**	0.00043
LYPLA2	Lysophospholipase II	Lipid metabolism	20.83	0.60	**34.93**	0.0024
SH3BGRL3	SH3 domain binding glutamate rich protein like 3	Redox homeostasis	43.63	1.30	**33.68**	0.00043
CD52	CD52 molecule	Respiratory burst, T cell receptor signaling	19.91	0.60	**32.93**	0.00043
ZDHHC18	Zinc finger DHHC-type containing 18	Posttranslational modification	15.60	0.49	**32.09**	0.00043
SYTL1	Synaptotagmin like 1	Exocytosis	4043.20	137.35	**29.44**	0.00043
RAB42	RAB42, member RAS oncogene family	GTPase activity, GTP binding	11.91	0.44	**27.17**	0.0069

Table 2: 20 genes with the lowest expression levels in ARMD compared to OA tissue. Gene expression levels in adverse reaction to metal debris (ARMD) and osteoarhtritis (OA) samples are listed as reads per kilobase million (RPKM) values, and the differences as fold changes (FCs). *p*-values are adjusted by false discovery rate (FDR).

Gene	Name	Function	RPKM (ARMD)	RPKM (OA)	FC	adj. *p*
UCK2	Uridine-cytidine kinase 2	Pyrimidine metabolism	4.66	1387.25	**-297.99**	0.00043
GDF5	Growth differentiation factor 5	Bone and cartilage development	0.15	19.56	**-131.23**	0.014
GPD1	Glycerol-3-phosphate dehydrogenase 1	Carbohydrate and lipid metabolism	0.18	22.04	**-122.14**	0.00043
ADH1B	Alcohol dehydrogenase 1B (class I), beta polypeptide	Alcohol metabolism	0.22	21.45	**-98.64**	0.00043
SCUBE1	Signal peptide, CUB domain and EGF like domain containing 1	Thrombosis and inflammation	0.22	14.25	**-63.50**	0.0008
TMEM196	Transmembrane protein 196	Regulation of cell proliferation	0.41	17.98	**-43.38**	0.00043
SCRG1	Stimulator of chondrogenesis 1	Chondrogenesis	6.64	268.27	**-40.39**	0.00043
NTRK2	Neurotrophic receptor tyrosine kinase 2	Neuron development	0.63	20.82	**-32.81**	0.00043
AMTN	Amelotin	Cell adhesion	3.89	123.23	**-31.67**	0.00043
SEMA3A	Semaphorin 3A	Inhibition of angiogenesis	0.48	13.97	**-28.96**	0.00043
ZNF385B	Zinc finger protein 385B	Apoptosis	1.01	28.69	**-28.48**	0.00043
FGF10	Fibroblast growth factor 10	Skeletal system development	1.94	53.45	**-27.57**	0.00043
DLX4	Distal-less homeobox 4	Regulation of transcription	0.94	25.10	**-26.79**	0.00739
GPR1	G protein-coupled receptor 1	G protein coupled receptor activity	2.34	58.64	**-25.08**	0.00043
CA9	Carbonic anhydrase 9	Cell proliferation	2.30	56.10	**-24.35**	0.00043
SLPI	Secretory leukocyte peptidase inhibitor	Immune response	9.51	222.85	**-23.43**	0.00043
CLIC5	Chloride intracellular channel 5	Chloride transport	1.58	35.39	**-22.34**	0.00043
SMOC1	SPARC related modular calcium binding 1	Skeletal system development	3.06	62.38	**-20.38**	0.00043
STAC2	SH3 and cysteine rich domain 2	Metal ion binding	0.54	10.61	**-19.76**	0.00043
SGCA	Sarcoglycan alpha	Muscle development	1.23	23.14	**-18.82**	0.0008
DLX3	Distal-less homeobox 3	Blood vessel development	1.20	21.90	**-18.31**	0.00043
RASD1	Ras related dexamethasone induced 1	Regulation of cell proliferation	4.38	79.12	**-18.08**	0.00043

When functions of the genes with FC > 2.0 were studied using the GO database (Table 3), functional categories involved immune response, macrophage and lymphocyte activation, cell adhesion, skeletal system development and several leukocyte signaling pathways (such as PI3KR1, phospholipase C, tyrosine kinase and integrin signaling). Additionally, Table 4 shows significant inflammatory and hypoxia-related genes which were expressed at higher level in ARMD than OA tissue.

When interactions between the most strongly up- and downregulated (FC > 10) genes were investigated, PRKACB, CD2, CD52 and CD53 were identified as potential central regulators of the observed changes in gene expression. The interaction network also contained the immunoglobulin receptor genes FCGR2A, FCGF2B and FCER1G. Another, smaller network was centered on the pentose phosphate shunt -related gene phosphogluconate dehydrogenase (PGD), and yet another on aggrecan (ACAN) (Figure 1).

Table 3: GO terms covering genes with significantly altered expression in ARMD vs OA tissue. Genes with an expression fold change (FC) > 2.0 in either direction were studied with the DAVID tool using the Gene Ontology (GO) database, and the resulting list of terms was reduced with REVIGO. *p*-values are corrected by false discovery rate (FDR).

Term	Number of altered genes	Total number of genes in the term	adj. *p*
Inflammatory response	110	407	6.74E-21
Cell adhesion	117	751	1.21E-17
Signal transduction	199	4491	2.30E-10
Adaptive immune response	43	194	4.68E-07
Cell-cell signaling	59	338	5.94E-06
Cell surface receptor signaling pathway	62	1997	8.90E-06
T cell costimulation	28	73	1.09E-05
Integrin-mediated signaling pathway	32	77	1.33E-05
Positive regulation of protein kinase B signaling	29	89	1.50E-05
Negative chemotaxis	17	34	9.47E-05
Transmembrane receptor protein tyrosine kinase signaling pathway	30	481	9.88E-05
Extracellular matrix organization	47	292	0.0001
Response to lipopolysaccharide	35	260	0.00025
Positive regulation of GTPase activity	98	629	0.00035
Negative regulation of axon extension involved in axon guidance	14	230	0.00071
Aging	46	291	0.00097
Positive regulation of interleukin-1 beta secretion	13	26	0.0011
Positive chemotaxis	16	33	0.0011
Positive regulation of cytosolic calcium ion concentration	35	235	0.0024
Cellular defense response	21	56	0.0027
Semaphorin-plexin signaling pathway	15	22	0.0031
Positive regulation of cell proliferation	81	832	0.015
Angiogenesis	46	245	0.016
Positive regulation of peptidyl-tyrosine phosphorylation	24	166	0.023
Platelet activation	29	108	0.023
Leukocyte migration	30	284	0.026
Proton transport	17	130	0.032
Cellular response to interleukin-1	23	67	0.033
Positive regulation of phosphatidylinositol 3-kinase signaling	20	64	0.033
Skeletal system development	32	155	0.038
Activation of phospholipase C activity	12	25	0.043
Protein localization to cell surface	11	23	0.0478

Table 4: Inflammatory and hypoxia-related genes with higher expression in ARMD compared to OA tissue. Gene expression levels are listed as reads per kilobase million (RPKM) values, and the differences as fold changes (FCs). *p*-values are adjusted by false discovery rate (FDR).

Gene	Name	Function	RPKM (ARMD)	RPKM (OA)	FC	adj. *p*
Inflammatory genes						
S100A9	S100 calcium binding protein A9	Innate immunity	662.78	42.13	**15.73**	0.00043
FCGR2B	Fc fragment of IgG receptor IIb	Adaptive immune response	17.80	1.30	**13.67**	0.00043
IL2RA	Interleukin 2 receptor subunit alpha	Lymphocyte activation	10.14	1.55	**6.54**	0.00043
IL18	Interleukin 18	Immune response	118.70	27.13	**4.37**	0.00043
TNFSF13B	TNF superfamily member 13b	Lymphocyte proliferation and activation	17.14	4.74	**3.62**	0.00043
SPN	Sialophorin	T cell activation	38.79	12.96	**2.99**	0.00043
IRF8	interferon regulatory factor 8	Interferon-mediated immune response	16.00	5.49	**2.91**	0.00043
CCL2	C-C motif chemokine ligand 2	Inflammation, monocyte chemotaxis	16.61	6.07	**2.74**	0.00043
CCL13	C-C motif chemokine ligand 13	Lymphocyte and monocyte chemotaxis	27.02	9.93	**2.72**	0.00043
CCL18	C-C motif chemokine ligand 18	Lymphocyte chemotaxis	137.69	50.68	**2.72**	0.00043
CCR7	C-C motif chemokine receptor 7	Leukocyte activation and chemotaxis	18.95	7.31	**2.59**	0.00043
CD7	CD7 molecule	Lymphocyte activation	11.12	4.45	**2.50**	0.00043
IL27RA	Interleukin 27 receptor subunit alpha	T cell activation	9.18	3.86	**2.38**	0.00043
FCAR	Fc fragment of IgA receptor	IgA-mediated immunity	10.28	4.50	**2.29**	0.00043
TNFSF14	TNF superfamily member 14	T cell activation	68.91	30.37	**2.27**	0.00043
ZAP70	Zeta chain of T cell receptor associated protein kinase 70	Lymphocyte activation	133.38	62.73	**2.13**	0.00043
CD8A	CD8a molecule	Tc cell activation	31.41	15.10	**2.08**	0.0083
CD8B	CD8b molecule	Tc cell activation	22.48	10.82	**2.08**	0.00043
IL1B	Interleukin 1 beta	Systemic inflammation	60.34	29.12	**2.07**	0.00043
CD40	CD40 molecule	Lymphocyte activation	16.37	8.06	**2.03**	0.00043
Hypoxia-related genes						
HMOX1	Heme oxygenase 1	Widespread response to hypoxia	523.17	72.32	**7.17**	0.00043
GSTO1	Glutathione S-transferase omega 1	Prevention of oxidative injury	411.06	60.58	**6.79**	0.00043
ASCL2	Achaete-scute family bHLH transcription factor 2	Response to hypoxia, HIF1A pathway	327.59	68.85	**4.76**	0.00043
TXNRD1	Thioredoxin reductase 1	Prevention of oxidative injury, Nrf2 pathway	84.50	20.76	**4.07**	0.00043
PRKCB	Protein kinase C beta	Response to hypoxia	26.71	8.82	**3.03**	0.00043
EGLN3	Egl-9 family hypoxia inducible factor 3	Apoptosis, regulation of cell proliferation	31.72	11.33	**2.81**	0.00043
NQO1	NAD(P)H quinone dehydrogenase 1	Redox homeostasis, NO biosynthesis	31.52	11.99	**2.63**	0.00043
SOD2	Superoxide dismutase 2	Superoxide detoxification	356.58	135.92	**2.62**	0.00043
GPX4	Glutathione peroxidase 4	Prevention of oxidative injury	10.67	4.35	**2.45**	0.00043
CXCR4	C-X-C motif chemokine receptor 4	Response to hypoxia, HIF1A pathway	8.27	4.00	**2.07**	0.00043

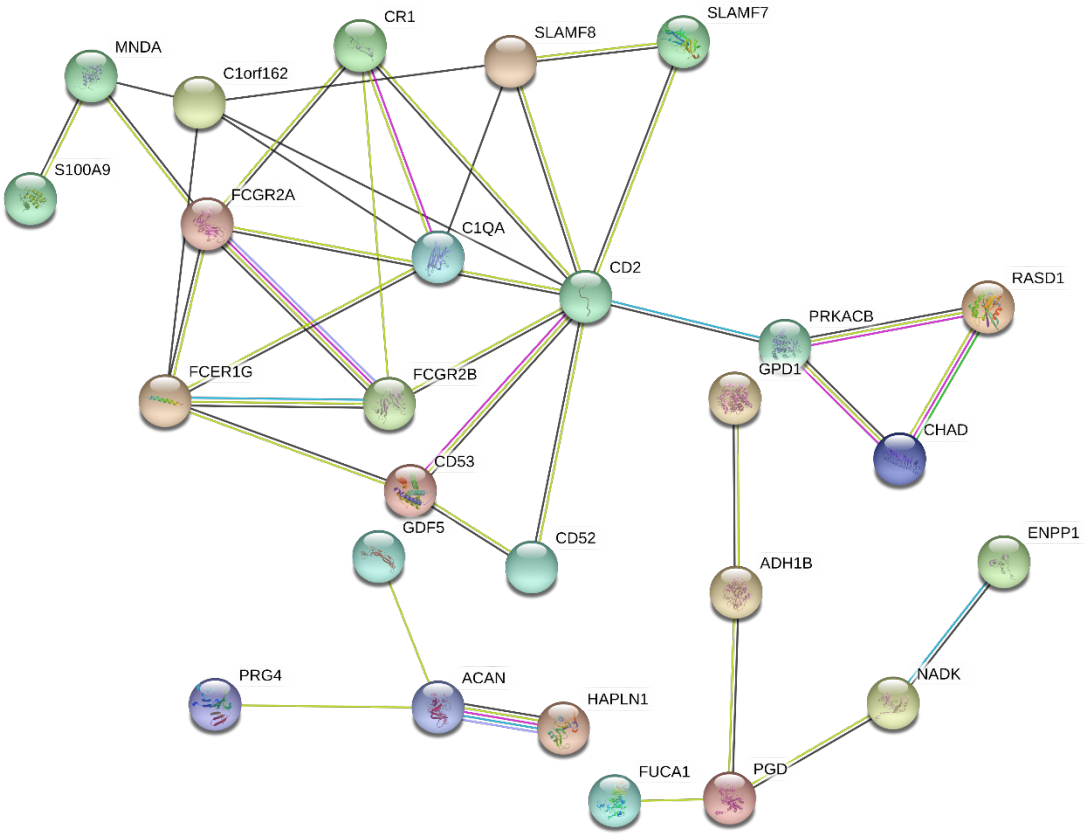

Figure 1: Interactions among the genes with greatest expression fold change in ARMD vs OA tissue. Genes with expression fold change (FC) > 10 in adverse reaction to metal debris (ARMD) vs osteoarthritis (OA) tissue were studied with STRING. Genes with no more than 2 interactions are excluded from the graph. Colors of the edges: green = activation, blue = binding, black = chemical reaction, red = inhibition, violet = catalysis, pink = posttranslational modification, yellow = transcriptional regulation, grey = other interaction.

Next, we compared tissue from ARMD reaction to the inflammatory pseudosynovial tissue from a failed MoP joint. In these cases, the differences in gene expression were less pronounced: the expression of 16 genes was significantly higher (Table 5) and 21 significantly lower (Table 6) in the ARMD reaction. All of these genes had a FC of more than 2.0 into either direction. Interestingly, the expression of genes central to myofibroblast (AEBP1 and DES) and osteoclast (CCL21, TREM2 and CKB) development was higher in MoP tissue.

When studying the interactions of the genes which were differentially expressed between ARMD and MoP tissues (Figure 2), IL8, NQO1, GSTT1 and HMOX1 were found to occupy central positions in the network, suggesting them as potential central regulators of the observed changes.

Table 5: Genes with significantly higher expression in ARMD than in MoP tissue. Gene expression levels in adverse reaction to metal debris (ARMD) and metal-on-plastic (MoP) samples are listed as reads per kilobase million (RPKM) values, and the differences as fold changes (FCs). *p*-values are adjusted by false discovery rate (FDR).

Gene	Name	Function	RPKM (ARMD)	RPKM (MoP)	FC	adj. *p*
RNF170	Ring finger protein 170	Protein ubiquitionation, metal ion binding	165.93	3.21	**51.77**	0.0085
TRIM25	Tripartite motif containing 25	Immune response	105.81	5.25	**20.16**	0.0085
FAM89A	Family with sequence similarity 89 member A	?	167.50	10.55	**15.88**	0.0085
SCRIB	Scribbled planar cell polarity protein	Regulation of cell proliferation, apoptosis	99.17	8.92	**11.12**	0.0085
CPSF1	Cleavage and polyadenylation specific factor 1	mRNA processing	125.18	11.94	**10.49**	0.0085
STMN1	Stathmin 1	Signal transduction	128.25	19.43	**6.60**	0.0085
CCL8	C-C motif chemokine ligand 8	Immune response	25.81	5.36	**4.81**	0.023
NOP56	NOP56 ribonucleoprotein	rRNA processing	135.68	32.39	**4.19**	0.0085
SLC40A1	Solute carrier family 40 member 1	Metal ion transport	168.55	40.79	**4.13**	0.0085
NQO1	NAD(P)H quinone dehydrogenase 1	Redox homeostasis, NO biosynthesis	31.52	9.24	**3.41**	0.0085
FGFBP2	Fibroblast growth factor binding protein 2	Tc cell -mediated immunity?	62.22	20.04	**3.10**	0.019
HMOX1	Heme oxygenase 1	Redox and metal ion homeostasis	523.17	187.11	**2.80**	0.014
CLEC5A	C-type lectin domain containing 5A	Immune response	29.03	10.55	**2.75**	0.0085
IL8	Interleukin 8	Chemotaxis, Immune response	65.98	26.19	**2.52**	0.014
EGLN3	Egl-9 family hypoxia inducible factor 3	Apoptosis, regulation of cell proliferation	31.72	12.59	**2.52**	0.0085
MGST1	Microsomal glutathione S-transferase 1	Redox homeostasis	57.59	23.96	**2.40**	0.024

Table 6: Genes with significantly lower expression in ARMD than MoP tissue. Gene expression levels in adverse reaction to metal debris (ARMD) and metal-on-plastic (MoP) samples are listed as reads per kilobase million (RPKM) values, and the differences as fold changes (FCs). *p*-values are adjusted by false discovery rate (FDR).

Gene	Name	Function	RPKM (ARMD)	RPKM (MoP)	FC	adj. *p*
ACTA1	actin, alpha 1, skeletal muscle	Cell structure	5.02	215.18	**-42.90**	0.0085
DES	desmin	Cell structure, myofibroblast development	5.14	117.74	**-22.90**	0.0085
HLA-B	major histocompatibility complex, class I, B	Immune response	4.44	38.73	**-8.72**	0.036
HLA-DRA	major histocompatibility complex, class II, DR alpha	Immune response	11.15	78.83	**-6.85**	0.024
SERPINA3	serpin family A member 3	Inflammatory response	13.54	70.71	**-5.22**	0.0085
CCL21	C-C motif chemokine ligand 21	T cell chemotaxis, osteoclast development	17.69	87.55	**-4.95**	0.024
RPS28	ribosomal protein S28	Ribosome component	110.94	406.39	**-3.66**	0.0085
CHI3L1	chitinase 3 like 1 (=YKL-40)	Inflammatory response	118.76	407.95	**-3.44**	0.0085
TPSB2	tryptase beta 2	Proteolysis	17.79	57.86	**-3.25**	0.047
PTGES	prostaglandin E synthase	Inflammatory response	14.36	43.64	**-3.04**	0.014
GSTT1	glutathione S-transferase theta 1	Redox homeostasis	27.14	81.94	**-3.02**	0.023
MT1E	metallothionein	Metal ion binding	109.39	319.36	**-2.92**	0.0085
RBP4	retinol binding protein 4	Glucose metabolism	93.62	262.29	**-2.80**	0.0085
TREM2	triggering receptor expressed on myeloid cells 2	Immune response, osteoclast development	133.31	347.37	**-2.61**	0.023
S100A8	S100 calcium binding protein A8	Inflammatory response	145.95	377.50	**-2.59**	0.024
AEBP1	AE binding protein 1	Skeletal system development, myofibroblast development	556.55	1431.68	**-2.57**	0.024
CKB	creatine kinase B	Energy homeostasis, osteoclast development	25.85	65.07	**-2.52**	0.24
TNC	tenascin C	ECM organization	41.74	97.90	**-2.35**	0.039
LPL	lipoprotein lipase	Lipid metabolism	11.17	27.44	**-2.34**	0.0141
GGT5	gamma-glutamyltransferase 5	Redox homeostasis, inflammatory response	23.00	53.56	**-2.33**	0.019
COX6B1	cytochrome c oxidase subunit 6B1	Redox metabolism	80.79	185.80	**-2.30**	0.032

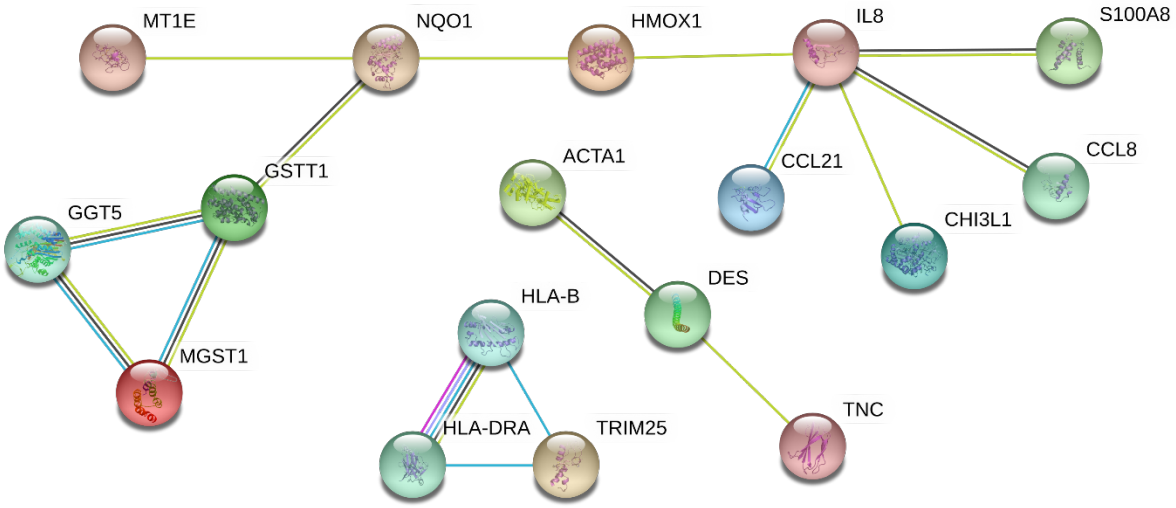

Figure 2: Interactions among the genes that were differentially expressed in ARMD vs MoP tissue. Significantly up- and downregulated genes in ARMD vs OA tissue were studied with STRING. Genes with no interactions are excluded from the graph. Colors of the edges: green = activation, blue = binding, black = chemical reaction, red = inhibition, violet = catalysis, pink = posttranslational modification, yellow = transcriptional regulation, grey = other interaction.

Discussion

When the pseudosynovial ARMD tissue from failed MoM implants was compared to synovial tissue from OA joints, a major difference in the gene expression profile was found while the differences between the ARMD reaction and the inflammatory reaction around failed MoP joints were less pronounced. Although these control tissues, i.e. OA synovium and MoP tissue, are not ideal in all aspects (though probably the best available), this study is the first attempt to understand the pathogenesis of the ARMD reaction by applying genome-wide expression analysis.

The list of genes with markedly different expression levels in ARMD and OA samples was found to contain a large number of genes involved in inflammatory response, cell proliferation, cellular metabolism and apoptosis. The inflammatory genes appear to be dominated by those involved in macrophage and lymphocyte-mediated responses, including several cytokines and chemokines, fitting to the current conception of the ARMD response [6,13,32]. Accordingly, functional categories (GO terms) included several leukocyte signaling pathways such as phospholipase C, PI3K and tyrosine kinase signaling.

Among the genes with largest differences in expression between ARMD and OA tissue, an interaction network centered on clusters of differentiation (CDs) CD2, CD52, CD53 and PRKACB (all strongly upregulated in ARMD samples) was discovered in the STRING analysis. Of these, CD2, CD52 and CD53 transduce signals from T cell receptors [33,34], and might thus mediate lymphocyte-mediated hypersensitivity reactions to metals. The immunoglobulin receptor genes FCGR2A, FCGR2B and FCER1G (also identified in the STRING analysis) may also participate in these reactions. However, as far as we know, no previous information about the role of any of these genes in ARMD reaction has been published. PRKACB is a serine/threonine protein kinase mediating cAMP signaling, with subsequent effects on a wide range of cellular processes, including proliferation, differentiation and inflammation [35,36]. Another, smaller network is centered on the pentose phosphate shunt -related gene phosphogluconate dehydrogenase (PGD), and includes genes related to carbohydrate, lipid and alcohol metabolism. Yet another network was found to be focused on aggrecan (ACAN), and included proteoglycan 4 (PRG4), growth and differentiation factor 5 (GDF5) and hyaluronan and

proteoglycan link protein 1 (HAPLN1). These genes, traditionally most strongly associated with cartilage metabolism, also seem to be expressed at lower levels in other tissues [37]. All of these genes were higher in OA synovium than in ARMD tissue, possibly reflecting compensatory increased synthesis of extracellular matrix (ECM) components in fibrotic synovial tissue typical for advanced OA [38].

The pathogenesis of the ARMD reaction is thought to be driven by metal ions and particles derived from MoM implants [8,39]. These implants are made of cobalt-chromium alloys, with other metals such as molybdenum and tungsten present in smaller amounts [40]. Due to their very high specific strength and corrosion resistance, these alloys were initially thought to be ideal for biomedical applications [41]. However, especially when subjected to large mechanical stress and "edge loading" (head-cup contact patch extending over the cup rim), significant amounts of metal particles can be abraded from MoM implants into the surrounding tissues [8,42]. Cobalt nanoparticles and Co(II) and Cr(VI) ions appear to be especially toxic, with chromium particles and Cr(III) ions only becoming harmful at markedly greater concentrations [43,44]. In the literature, the biochemical mechanisms of cobalt-induced toxicity appear to be more comprehensively characterized than those of chromium. In addition, cobalt may activate macrophages directly through TLR4 [17]. It also modifies macrophage phenotype [45] and causes strong oxidative stress [46].

Cobalt is known to mimic hypoxic conditions in cells, inhibiting the degradation of the transcription factor hypoxia-inducible factor 1 alpha (HIF1A) in the proteasome [47] and, accordingly, high expression of hypoxia-related genes was observed in ARMD samples. These genes include heme oxygenase 1 (HMOX1), NADPH quinone dehydrogenase 1 (NQO1), Egl-9 family hypoxia inducible factor 3 (EGLN3) and superoxide dismutase 2 (SOD2). HIF1A mRNA levels were not significantly different in either comparison. This was however expected, as hypoxia (as well as cobalt) is known to enhance HIF1A expression by inhibiting the degradation of the protein, not by affecting on transcription. Accordingly, enhanced HIF1A protein levels have been detected in ARMD tissue [18] and in macrophages exposured to cobalt [45]. In conclusion, the present results support the hypoxia mimicry hypothesis as a contributing factor in AMRD, but further studies are needed to understand the pathogenetic mechanisms in detail.

When comparing gene expression in ARMD tissue to that in the inflammatory tissue around failed MoP joints, a relatively small number of significantly up- or downregulated genes were identified. This suggests that the pathophysiologies of these two reactions hold many similarities. Indeed, both reactions are thought to be particle driven, the other by polyethylene debris and the other by metal debris. Alarmins, endogenous factors that promote noninfective inflammation, may serve as an example of mechanisms involved in both responses. As compared to OA samples, ARMD tissue expressed increased levels of S100 calcium-binding protein A9 (S100A9), an alarmin that heterodimerizes with S100A8 to form calprotectin [48]. MoP tissue expressed S100A9 at equally high levels and in addition, the expression of S100A8 was higher in MoP than in ARDM tissue. Alarmin S100A8/S100A9 has been associated with a wide variety of inflammatory conditions, from arthritis [49] to lung injury [50]. In previous studies, alarmins in general have been linked to aseptic implant loosening [51,52]. Further studies are needed to understand their detailed role in the pathogenesis of the response.

There were also significant differences in the gene expression profiles between ARMD and MoP tissues that may provide insights into the mechanisms of the two reaction types. Among the genes upregulated in ARMD tissue compared to MoP, there were, perhaps expectedly, several associated with metal ion binding and redox homeostasis. These include ring finger protein 170 (RNF170), solute carrier family 40 member 1 (SLC40A1) and heme oxygenase 1 (HMOX1). The last of these is especially interesting, as it is a cytoprotective factor induced during hypoxia [53]. HMOX1 mediates heme catabolism [54], but also regulates the inflammatory response by inhibiting the activation and nuclear translocation of the inflammatory transcription factor NF-κB and by enhancing the production of anti-inflammatory cytokines [55]. Along with HMOX1, NAD(P)H quinone dehydrogenase (NQO1) and microsomal glutathione S-transferase 1 (MGST1) [56] (which were both enhanced in ARMD tissue) are likely compensatory mechanisms to combat the oxidative stress induced by metal ions.

List of the genes, which were higher in MoP than ARMD tissue contained also a number of inflammatory genes. These genes appear to be widely expressed by both macrophages and lymphocytes, and thus provide

no specific information about the involvement of these cell types in the reaction. Interestingly, many genes stimulating the differentiation and functions of osteoclasts were more highly expressed in MoP tissue compared to ARMD. These include C-C motif chemokine ligand 21 (CCL21) [57], triggering receptor expressed on myeloid cells 2 (TREM2) [58] and creatine kinase B (CKB) [59]. Osteoclast-mediated bone resorption is a known feature of adverse reactions seen in MoM [60] and especially in MoP [22] joints, and polyethylene particles have been demonstrated to promote osteoclastic differentiation of mononuclear cells [61]. However, the precise roles of the aforementioned factors in these processes remain largely unknown. As far as we know, no comprehensive comparative analysis of gene expression in ARMD and MoP reactions has previously been published.

A possible weakness of the present study is that both ARMD and MoP samples were from around failed prostheses. This leaves open the possibility that part of the observed changes may be attributed to the normal tissue reaction following arthroplasty or to the particle driven reaction leading to implant failure in general, rather than specific metal (or plastic) debris evoked toxicity. An ideal control for ARMD tissue would have been pseudosynovial tissue from around a normally functioning MoM joint with no signs of ARMD. Obtaining such tissue from well-functioning joints is, however, not possible because there is no indication for revision surgery. In general, the present results should be interpreted considering these limitations.

The present results show that there is a widespread difference in gene expression between pseudosynovial ARMD tissue and synovial tissue from OA joint. In contrast, differences in gene expression between ARMD and MoP tissues were less pronounced and, interestingly, osteolytic genes were among those significantly upregulated in MoP tissue. The big picture, based on genome-wide expression analysis, shows that ARMD reaction has unique features including up-regulation of genes associated with redox homeostasis, metal ion binding and transport, lymphocyte and macrophage activation, cellular metabolism and apoptosis.

Acknowledgements

We wish to thank Mss. Meiju Kukkonen and Petra Miikkulainen for excellent technical assistance, as well as Mrs. Heli Määttä for skillful secretarial help.

Funding sources

The study was supported by the competitive research funding of Tampere University Hospital, Tampere, Finland.

References

[1] A. Eskelinen, V. Remes, I. Helenius, P. Pulkkinen, J. Nevalainen, P. Paavolainen, Total hip arthroplasty for primary osteoarthrosis in younger patients in the Finnish arthroplasty register. 4,661 primary replacements followed for 0-22 years, Acta Orthop. 76 (2005) 28–41. doi:10.1080/00016470510030292.

[2] M. Bhandari, M. Swiontkowski, Management of Acute Hip Fracture., N. Engl. J. Med. 377 (2017) 2053–2062. doi:10.1056/NEJMcp1611090.

[3] J.A. López-López, R.L. Humphriss, A.D. Beswick, H.H.Z. Thom, L.P. Hunt, A. Burston, C.G. Fawsitt, W. Hollingworth, J.P.T. Higgins, N.J. Welton, A.W. Blom, E.M.R. Marques, Choice of implant combinations in total hip replacement: systematic review and network meta-analysis, BMJ. (2017) j4651. doi:10.1136/bmj.j4651.

[4] A. Reito, L. Lehtovirta, O. Lainiala, K. Mäkelä, A. Eskelinen, Lack of evidence-the anti-stepwise introduction of metal-on-metal hip replacements., Acta Orthop. 88 (2017) 478–483. doi:10.1080/17453674.2017.1353794.

[5] S.-A.L. Ras Sørensen, H.L. Jørgensen, S.L. Sporing, J.B. Lauritzen, Revision rates for metal-on-metal hip resurfacing and metal-on-metal total hip arthroplasty – a systematic review, Hip Int. 26 (2016) 515–521. doi:10.5301/hipint.5000444.

[6] H.-G. Willert, G.H. Buchhorn, A. Fayyazi, R. Flury, M. Windler, G. Köster, C.H. Lohmann, Metal-on-metal bearings and hypersensitivity in patients with artificial hip joints. A clinical and histomorphological study, J. Bone Joint Surg. Am. 87 (2005) 28–36. doi:10.2106/JBJS.A.02039pp.

[7] M.H.L. Liow, Y.-M. Kwon, Metal-on-metal total hip arthroplasty: risk factors for pseudotumours and

clinical systematic evaluation., Int. Orthop. 41 (2017) 885–892. doi:10.1007/s00264-016-3305-1.

[8] H. Dahlstrand, A. Stark, M.C. Wick, L. Anissian, N.P. Hailer, R.J. Weiss, Comparison of metal ion concentrations and implant survival after total hip arthroplasty with metal-on-metal versus metal-on-polyethylene articulations, Acta Orthop. 88 (2017) 490–495. doi:10.1080/17453674.2017.1350370.

[9] A. Matthies, R. Underwood, P. Cann, K. Ilo, Z. Nawaz, J. Skinner, A.J. Hart, Retrieval analysis of 240 metal-on-metal hip components, comparing modular total hip replacement with hip resurfacing, J. Bone Joint Surg. Br. 93 (2011) 307–314. doi:10.1302/0301-620X.93B3.25551.

[10] H.S. Gill, G. Grammatopoulos, S. Adshead, E. Tsialogiannis, E. Tsiridis, Molecular and immune toxicity of CoCr nanoparticles in MoM hip arthroplasty., Trends Mol. Med. 18 (2012) 145–55. doi:10.1016/j.molmed.2011.12.002.

[11] H. Pandit, M. Vlychou, D. Whitwell, D. Crook, R. Luqmani, S. Ostlere, D.W. Murray, N.A. Athanasou, Necrotic granulomatous pseudotumours in bilateral resurfacing hip arthoplasties: evidence for a type IV immune response, Virchows Arch. An Int. J. Pathol. 453 (2008) 529–534. doi:10.1007/s00428-008-0659-9.

[12] K. Man, L.-H. Jiang, R. Foster, X.B. Yang, Immunological Responses to Total Hip Arthroplasty, J. Funct. Biomater. 8 (2017). doi:10.3390/jfb8030033.

[13] P. Campbell, E. Ebramzadeh, S. Nelson, K. Takamura, K. De Smet, H.C. Amstutz, Histological features of pseudotumor-like tissues from metal-on-metal hips, Clin. Orthop. Relat. Res. 468 (2010) 2321–2327. doi:10.1007/s11999-010-1372-y.

[14] S.B. Goodman, Wear particles, periprosthetic osteolysis and the immune system, Biomaterials. 28 (2007) 5044–5048. doi:10.1016/j.biomaterials.2007.06.035.

[15] G. Liu, T. Guo, Y. Zhang, N. Liu, J.J. Chen, J.J. Chen, J. Zhang, J. Zhao, Apoptotic pathways of macrophages within osteolytic interface membrane in periprosthestic osteolysis after total hip replacement, APMIS Acta Pathol. Microbiol. Immunol. Scand. 125 (2017) 565–578. doi:10.1111/apm.12679.

[16] A. Jonitz-Heincke, J. Tillmann, A. Klinder, S. Krueger, J.P. Kretzer, P.J. Høl, A.C. Paulus, R. Bader, The Impact of Metal Ion Exposure on the Cellular Behavior of Human Osteoblasts and PBMCs: In Vitro Analyses of Osteolytic Processes, Mater. (Basel, Switzerland). 10 (2017). doi:10.3390/ma10070734.

[17] L. Samelko, S. Landgraeber, K. McAllister, J. Jacobs, N.J. Hallab, TLR4 (not TLR2) dominate cognate TLR activity associated with CoCrMo implant particles, J. Orthop. Res. Off. Publ. Orthop. Res. Soc. 35 (2017) 1007–1017. doi:10.1002/jor.23368.

[18] L. Samelko, M.S. Caicedo, S.-J. Lim, C. Della-Valle, J. Jacobs, N.J. Hallab, Cobalt-alloy implant debris induce HIF-1α hypoxia associated responses: a mechanism for metal-specific orthopedic implant failure, PLoS One. 8 (2013) e67127. doi:10.1371/journal.pone.0067127.

[19] T. Fujishiro, D.J.F. Moojen, N. Kobayashi, W.J.A. Dhert, T.W. Bauer, Perivascular and diffuse lymphocytic inflammation are not specific for failed metal-on-metal hip implants, Clin. Orthop. Relat. Res. 469 (2011) 1127–1133. doi:10.1007/s11999-010-1649-1.

[20] T.D. Zaveri, N. V Dolgova, J.S. Lewis, K. Hamaker, M.J. Clare-Salzler, B.G. Keselowsky, Macrophage integrins modulate response to ultra-high molecular weight polyethylene particles and direct particle-induced osteolysis, Biomaterials. 115 (2017) 128–140. doi:10.1016/j.biomaterials.2016.10.038.

[21] O.N. Schipper, S.L. Haddad, P. Pytel, Y. Zhou, Histological Analysis of Early Osteolysis in Total Ankle Arthroplasty, Foot Ankle Int. 38 (2017) 351–359. doi:10.1177/1071100716682333.

[22] M. Sartori, F. Vincenzi, A. Ravani, S. Cepollaro, L. Martini, K. Varani, M. Fini, M. Tschon, RAW 264.7 co-cultured with ultra-high molecular weight polyethylene particles spontaneously differentiate into osteoclasts: an in vitro model of periprosthetic osteolysis, J. Biomed. Mater. Res. A. 105 (2017) 510–520. doi:10.1002/jbm.a.35912.

[23] M. Wolfien, C. Rimmbach, U. Schmitz, J.J. Jung, S. Krebs, G. Steinhoff, R. David, O. Wolkenhauer, TRAPLINE: a standardized and automated pipeline for RNA sequencing data analysis, evaluation and annotation, BMC Bioinformatics. 17 (2016) 21. doi:10.1186/s12859-015-0873-9.

[24] E. Afgan, D. Baker, M. van den Beek, D. Blankenberg, D. Bouvier, M. Čech, J. Chilton, D. Clements, N. Coraor, C. Eberhard, B. Grüning, A. Guerler, J. Hillman-Jackson, G. Von Kuster, E. Rasche, N. Soranzo, N. Turaga, J. Taylor, A. Nekrutenko, J. Goecks, The Galaxy platform for accessible, reproducible and collaborative biomedical analyses: 2016 update, Nucleic Acids Res. 44 (2016) W3–W10. doi:10.1093/nar/gkw343.

[25] D. Blankenberg, A. Gordon, G. Von Kuster, N. Coraor, J. Taylor, A. Nekrutenko, Manipulation of FASTQ data with Galaxy, Bioinformatics. 26 (2010) 1783–1785. doi:10.1093/bioinformatics/btq281.

[26] D. Kim, G. Pertea, C. Trapnell, H. Pimentel, R. Kelley, S.L. Salzberg, TopHat2: accurate alignment of transcriptomes in the presence of insertions, deletions and gene fusions, Genome Biol. 14 (2013) R36. doi:10.1186/gb-2013-14-4-r36.

[27] C. Trapnell, D.G. Hendrickson, M. Sauvageau, L. Goff, J.L. Rinn, L. Pachter, Differential analysis of gene regulation at transcript resolution with RNA-seq, Nat Biotechnol. 31 (2012). doi:10.1038/nbt.2450.

[28] M.A. Gene Ontology Consortium, J. Clark, A. Ireland, J. Lomax, M. Ashburner, R. Foulger, K. Eilbeck, S. Lewis, B. Marshall, C. Mungall, J. Richter, G.M. Rubin, J.A. Blake, C. Bult, M. Dolan, H. Drabkin, J.T. Eppig, D.P. Hill, L. Ni, M. Ringwald, R. Balakrishnan, J.M. Cherry, K.R. Christie, M.C. Costanzo, S.S. Dwight, S. Engel, D.G. Fisk, J.E. Hirschman, E.L. Hong, R.S. Nash, A. Sethuraman, C.L. Theesfeld, D. Botstein, K. Dolinski, B. Feierbach, T. Berardini, S. Mundodi, S.Y. Rhee, R. Apweiler, D. Barrell, E. Camon, E. Dimmer, V. Lee, R. Chisholm, P. Gaudet, W. Kibbe, R. Kishore, E.M. Schwarz, P. Sternberg, M. Gwinn, L. Hannick, J. Wortman, M. Berriman, V. Wood, N. de la Cruz, P. Tonellato, P. Jaiswal, T. Seigfried, R. White, Gene Ontology Consortium, The Gene Ontology (GO) database and informatics resource, Nucleic Acids Res. 32 (2004) 258D–261. doi:10.1093/nar/gkh036.

[29] D.W. Huang, B.T. Sherman, R.A. Lempicki, Systematic and integrative analysis of large gene lists using DAVID bioinformatics resources, Nat. Protoc. 4 (2009) 44–57. doi:10.1038/nprot.2008.211.

[30] F. Supek, M. Bošnjak, N. Škunca, T. Šmuc, REVIGO Summarizes and Visualizes Long Lists of Gene Ontology Terms, PLoS One. 6 (2011) e21800. doi:10.1371/journal.pone.0021800.

[31] D. Szklarczyk, A. Franceschini, S. Wyder, K. Forslund, D. Heller, J. Huerta-Cepas, M. Simonovic, A. Roth, A. Santos, K.P. Tsafou, M. Kuhn, P. Bork, L.J. Jensen, C. von Mering, STRING v10: protein–protein interaction networks, integrated over the tree of life, Nucleic Acids Res. 43 (2015) D452. doi:10.1093/nar/gku1003.

[32] E.-L. Paukkeri, R. Korhonen, M. Hämäläinen, M. Pesu, A. Eskelinen, T. Moilanen, E. Moilanen, The Inflammatory Phenotype in Failed Metal-On-Metal Hip Arthroplasty Correlates with Blood Metal Concentrations., PLoS One. 11 (2016) e0155121. doi:10.1371/journal.pone.0155121.

[33] J. Leitner, D. Herndler-Brandstetter, G.J. Zlabinger, B. Grubeck-Loebenstein, P. Steinberger, CD58/CD2 Is the Primary Costimulatory Pathway in Human CD28-CD8+ T Cells, J. Immunol. (Baltimore, Md. 1950). 195 (2015) 477–487. doi:10.4049/jimmunol.1401917.

[34] S.R. Mohan, M.J. Clemente, M. Afable, H.N. Cazzolli, N. Bejanyan, M.W. Wlodarski, A.E. Lichtin, J.P. Maciejewski, Therapeutic implications of variable expression of CD52 on clonal cytotoxic T cells in CD8+ large granular lymphocyte leukemia, Haematologica. 94 (2009) 1407–1414. doi:10.3324/haematol.2009.009191.

[35] L.V. Moen, Z. Sener, R. Volchenkov, A.C. Svarstad, A.M. Eriksen, H.L. Holen, B.S. Skålhegg, Ablation of the Cβ2 subunit of PKA in immune cells leads to increased susceptibility to systemic inflammation in mice, Eur. J. Immunol. 47 (2017) 1880–1889. doi:10.1002/eji.201646809.

[36] J.M. Steichen, G.H. Iyer, S. Li, S.A. Saldanha, M.S. Deal, V.L. Woods, S.S. Taylor, Global consequences of activation loop phosphorylation on protein kinase A, J. Biol. Chem. 285 (2010) 3825–3832. doi:10.1074/jbc.M109.061820.

[37] L. Fagerberg, B.M. Hallström, P. Oksvold, C. Kampf, D. Djureinovic, J. Odeberg, M. Habuka, S. Tahmasebpoor, A. Danielsson, K. Edlund, A. Asplund, E. Sjöstedt, E. Lundberg, C.A.-K. Szigyarto, M. Skogs, J.O. Takanen, H. Berling, H. Tegel, J. Mulder, P. Nilsson, J.M. Schwenk, C. Lindskog, F. Danielsson, A. Mardinoglu, Å. Sivertsson, K. von Feilitzen, M. Forsberg, M. Zwahlen, I. Olsson, S. Navani, M. Huss, J. Nielsen, F. Ponten, M. Uhlén, Analysis of the Human Tissue-specific Expression by Genome-wide Integration of Transcriptomics and Antibody-based Proteomics, Mol. Cell. Proteomics. 13 (2014) 397–406. doi:10.1074/mcp.M113.035600.

[38] T. Hardingham, Extracellular matrix and pathogenic mechanisms in osteoarthritis, Curr. Rheumatol. Rep. 10 (2008) 30–36. doi:10.1007/s11926-008-0006-9.

[39] P.A. Revell, Biological causes of prosthetic joint failure*Note: This chapter is an updated version of Chapter 15 from the first edition of Joint replacement technology edited by P. A. Revell and published by Woodhead Publishing 2008*, in: Jt. Replace. Technol., Elsevier, 2014: pp. 298–369. doi:10.1533/9780857098474.3.298.

[40] T.M. Devine, F.J. Kummer, J. Wulff, Wrought cobalt-chromium surgical implant alloys, J. Mater. Sci. 7 (1972) 126–128. doi:10.1007/BF00549560.

[41] D.J.S. Hyslop, A.M. Abdelkader, A. Cox, D.J. Fray, Electrochemical synthesis of a biomedically important Co–Cr alloy, Acta Mater. 58 (2010) 3124–3130. doi:10.1016/j.actamat.2010.01.053.

[42] R.J. Underwood, A. Zografos, R.S. Sayles, A. Hart, P. Cann, Edge loading in metal-on-metal hips: low

clearance is a new risk factor., Proc. Inst. Mech. Eng. H. 226 (2012) 217–26. doi:10.1177/0954411911431397.

[43] M. Akbar, J.M. Brewer, M.H. Grant, Effect of chromium and cobalt ions on primary human lymphocytes *in vitro*, J. Immunotoxicol. 8 (2011) 140–149. doi:10.3109/1547691X.2011.553845.

[44] Y.-M. Kwon, Z. Xia, S. Glyn-Jones, D. Beard, H.S. Gill, D.W. Murray, Dose-dependent cytotoxicity of clinically relevant cobalt nanoparticles and ions on macrophages in vitro., Biomed. Mater. 4 (2009) 25018. doi:10.1088/1748-6041/4/2/025018.

[45] M. Kumanto, E.-L. Paukkeri, R. Nieminen, E. Moilanen, Cobalt(II) Chloride Modifies the Phenotype of Macrophage Activation, Basic Clin. Pharmacol. Toxicol. 121 (2017) 98–105. doi:10.1111/bcpt.12773.

[46] K. Jomova, M. Valko, Advances in metal-induced oxidative stress and human disease, Toxicology. 283 (2011) 65–87. doi:10.1016/j.tox.2011.03.001.

[47] A. Nyga, A. Hart, T.D. Tetley, Importance of the HIF pathway in cobalt nanoparticle-induced cytotoxicity and inflammation in human macrophages, Nanotoxicology. 9 (2015) 905–917. doi:10.3109/17435390.2014.991430.

[48] F.S. Lehmann, E. Burri, C. Beglinger, The role and utility of faecal markers in inflammatory bowel disease, Therap. Adv. Gastroenterol. 8 (2015) 23–36. doi:10.1177/1756283X14553384.

[49] J. Austermann, S. Zenker, J. Roth, S100-alarmins: potential therapeutic targets for arthritis, Expert Opin. Ther. Targets. 21 (2017) 738–750. doi:10.1080/14728222.2017.1330411.

[50] D. Chakraborty, S. Zenker, J. Rossaint, A. Hölscher, M. Pohlen, A. Zarbock, J. Roth, T. Vogl, Alarmin S100A8 Activates Alveolar Epithelial Cells in the Context of Acute Lung Injury in a TLR4-Dependent Manner., Front. Immunol. 8 (2017) 1493. doi:10.3389/fimmu.2017.01493.

[51] Y. Tamaki, Y. Takakubo, K. Goto, T. Hirayama, K. Sasaki, Y.T. Konttinen, S.B. Goodman, M. Takagi, Increased expression of toll-like receptors in aseptic loose periprosthetic tissues and septic synovial membranes around total hip implants., J. Rheumatol. 36 (2009) 598–608. doi:10.3899/jrheum.080390.

[52] L. Samelko, S. Landgraeber, K. McAllister, J. Jacobs, N.J. Hallab, Cobalt Alloy Implant Debris Induces Inflammation and Bone Loss Primarily through Danger Signaling, Not TLR4 Activation: Implications for DAMP-ening Implant Related Inflammation, PLoS One. 11 (2016) e0160141. doi:10.1371/journal.pone.0160141.

[53] J.A. Neubauer, J. Sunderram, Heme oxygenase-1 and chronic hypoxia, Respir. Physiol. Neurobiol. 184 (2012) 178–185. doi:10.1016/j.resp.2012.06.027.

[54] M. Exner, E. Minar, O. Wagner, M. Schillinger, The role of heme oxygenase-1 promoter polymorphisms in human disease, Free Radic. Biol. Med. 37 (2004) 1097–1104. doi:10.1016/J.FREERADBIOMED.2004.07.008.

[55] C.A. Piantadosi, C.M. Withers, R.R. Bartz, N.C. MacGarvey, P. Fu, T.E. Sweeney, K.E. Welty-Wolf, H.B. Suliman, Heme Oxygenase-1 Couples Activation of Mitochondrial Biogenesis to Anti-inflammatory Cytokine Expression, J. Biol. Chem. 286 (2011) 16374–16385. doi:10.1074/jbc.M110.207738.

[56] J. Shi, H.L. Karlsson, K. Johansson, V. Gogvadze, L. Xiao, J. Li, T. Burks, A. Garcia-Bennett, A. Uheida, M. Muhammed, S. Mathur, R. Morgenstern, V.E. Kagan, B. Fadeel, Microsomal glutathione transferase 1 protects against toxicity induced by silica nanoparticles but not by zinc oxide nanoparticles, ACS Nano. 6 (2012) 1925–1938. doi:10.1021/nn2021056.

[57] J. Lee, C. Park, H.J. Kim, Y.D. Lee, Z.H. Lee, Y.W. Song, H.-H. Kim, Stimulation of osteoclast migration and bone resorption by C-C chemokine ligands 19 and 21, Exp. Mol. Med. 49 (2017) e358. doi:10.1038/emm.2017.100.

[58] M.B. Humphrey, M.R. Daws, S.C. Spusta, E.C. Niemi, J.A. Torchia, L.L. Lanier, W.E. Seaman, M.C. Nakamura, TREM2, a DAP12-associated receptor, regulates osteoclast differentiation and function, J. Bone Miner. Res. Off. J. Am. Soc. Bone Miner. Res. 21 (2006) 237–245. doi:10.1359/JBMR.051016.

[59] E.-J. Chang, J. Ha, F. Oerlemans, Y.J. Lee, S.W. Lee, J. Ryu, H.J. Kim, Y. Lee, H.-M. Kim, J.-Y. Choi, J.Y. Kim, C.S. Shin, Y.K. Pak, S. Tanaka, B. Wieringa, Z.H. Lee, H.-H. Kim, Brain-type creatine kinase has a crucial role in osteoclast-mediated bone resorption, Nat. Med. 14 (2008) 966–972. doi:10.1038/nm.1860.

[60] L. Dong, R. Wang, Y.-A. Zhu, C. Wang, H. Diao, C. Zhang, J. Zhao, J. Zhang, Antisense oligonucleotide targeting TNF-alpha can suppress Co-Cr-Mo particle-induced osteolysis, J. Orthop. Res. Off. Publ. Orthop. Res. Soc. 26 (2008) 1114–1120. doi:10.1002/jor.20607.

[61] F. Veronesi, M. Tschon, M. Fini, Gene Expression in Osteolysis: Review on the Identification of Altered Molecular Pathways in Preclinical and Clinical Studies, Int. J. Mol. Sci. 18 (2017) 499. doi:10.3390/ijms18030499.